JCTC Journal of Chemical Theory and Computation

Stationary Points on the PES of *N*-Methoxy Peptides and Their Boron Isosteres: An Ab Initio Study

Alpeshkumar K. Malde, Santosh A. Khedkar, and Evans C. Coutinho*

Department of Pharmaceutical Chemistry, Bombay College of Pharmacy, Kalina, Santacruz (E), Mumbai 400 098, India

Received June 6, 2006

Abstract: The conformational space of *N*-methoxy-*N*-methylacetamide [$CH_3-CO-N(OCH_3)-CH_3$, NMA-NOM] and its boron isostere [$CH_3-CO-B(OCH_3)CH_3$, BMA-BOM] has been studied at the HF, B3LYP, and MP2 levels of theory with the 6-31+G* basis set. The minima, saddle points, and rotation barriers on the PES of these molecules have been located, and the energy barriers estimated. The *omega* rotation barrier is relatively lower in the boron isostere than in NMA-NOM. The difference in the rotation barrier has been attributed to second-order orbital interactions, like negative hyperconjugation, as revealed by NBO calculations. As an extension, *N*-acetyl-*N*′-methoxy-*N*′-methylamide of alanine (Ala-NOM) and its boron isostere (B-Ala-BOM) have been adopted as model peptides to study the conformational preferences about the ϕ and ψ torsion angles. The study reveals a strong preference for conformations of type-V beta turn and left-handed α-helix for Ala-NOM. B-Ala-BOM, on the other hand, favors conformations of type-Va beta turn, mirror image of Poly-L-Pro II helix, and structures with positive ϕ and extended ψ. The replacement of nitrogen by boron changes the electronic and conformational properties of the peptide, extends greater flexibility around the *omega* angle, induces a strong preference for positive *phi* values, and shifts the site of nucleophilic attack from the carbonyl group to boron.

Introduction

The biological effects of peptides and proteins are governed by their conformations. The values of the three backbone torsion angles—*omega* (ω), *phi* (ϕ), and *psi* (ψ)—dictate the secondary structure and hence the conformations of peptides.[1] Most natural peptides adopt ω with 180° (trans), and occasionally, ω assumes 0° (cis) for peptides with the Xxx-Pro and Xxx-Gly motifs.[2] The ϕ and ψ values in natural peptides and proteins are restricted to the allowed regions of the Ramachandran map.[1] Peptides form an important area of therapeutics,[3] e.g. insulin, gastric inhibitory polypeptide, substance P, thyrotropin releasing hormone, gastrin, growth hormone, bradykinin, etc. have important therapeutic applications. The advantages of using peptides as therapeutic agents are their high potency, selectivity, and specificity. The major obstacle is oral delivery due to degradation at the "scissile" amide bond. This is the reason peptides like insulin and thyrotropin cannot be given orally and have to be administered parenterally.

The major challenges in peptide therapeutics are confering potency, specificity, and selectivity to peptides designed from natural analogues for certain biological end points. Modifications of the amide bond and isosteric/bioisosteric replacements have been explored to address issues like selectivity toward a particular protein target, improving binding affinity, and stability toward proteolytic enzymes. N-Methylation;[4] N-hydroxylation;[5] replacement of the amide bond by sulfonamide, phosphonamidate, and carbamate;[6,7] reduction of the amide bond; inversion of stereochemistry at the alpha carbon; isosteric replacement of the carbonyl carbon with boron (peptide boronic acid[8,9]); and isosteric replacement of the alpha carbon with boron (ammonia-carboxyboranes[10−12]) have been reported as techniques to explore new peptide conformations and to design proteolytically stable, "druglike" molecules.

* Corresponding author phone: +91-22-26670871; fax: +91-22-26670816; e-mail: evans@bcpindia.org.

10.1021/ct600192g CCC: $33.50
Published on Web 09/14/2006

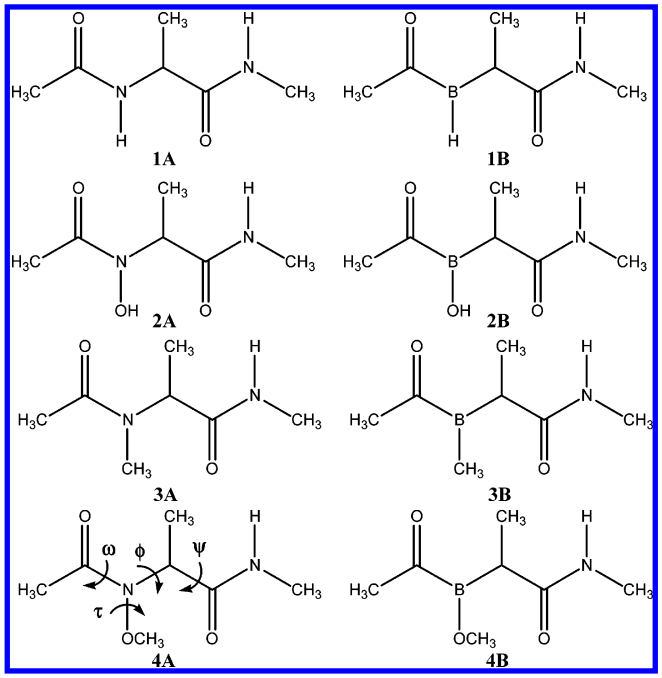

Figure 1. Structures of natural and the corresponding boron peptides.

We had reported for the first time a boron isostere of the amide nitrogen in peptides (Figure 1, **1A** and **1B**) and had studied the ω, ϕ, and ψ preferences by ab initio and density functional methods.[13,14] These molecules were designed as plausible serine protease inhibitors. The replacement of nitrogen with boron leads to two new characteristics: a preference of the ω angle for 90°, in contrast to 180° or 0° for natural peptides; and second, conformations that lie in the "disallowed regions" (positive ϕ angles) of the Ramachandran plot. These peptides also exhibit greater flexibility around the ω angle. However, these boron analogues are synthetically challenging. In a subsequent paper,[15] we had studied hydroxy derivatives of boron (Figure 1, **2B**) which are counterparts of the *N*-hydroxy derivatives of natural peptides (Figure 1, **2A**). The acylhydroxyboranes (Figure 1, **2B**) are more accessible synthetically than the acylboranes[13] (Figure 1, **1B**) designed earlier.

Another group of peptides are the *N*-methyl analogues (Figure 1, **3A**) which are seen naturally in sarcosine, actinomycin D, cyclosporin, etc.[16,17] and have also been exploited synthetically with the aim of imparting specific secondary structures (α-helix) to peptides.[18] The boron analogues of the *N*-methyl peptides are represented by **3B** in Figure 1. However, from a synthetic standpoint, the methoxy derivatives (Figure 1, **4B**) are much more accessible and stable over **3B**. *N*-methoxy peptides (Figure 1, **4A**) have received little attention from theoretical and experimental chemists and could offer new approaches of modulating the peptide backbone in novel folds.

In this paper, we look at the ω, ϕ, and ψ preferences of *N*-methoxy peptides (Figure 1, **4A**) and their boron isosteres (Figure 1, **4B**), by ab initio and density functional methods. To understand the preferences for the 'ω angle' in such peptides, *N*-methyl-*N*-methoxyacetamide (NMA-NOM, Figure 2 **5A**) and acetylmethylmethoxyborane (BMA-BOM, Figure 2 **5B**) have been established as models for **4A** and **4B**, respectively. *N*-Acetyl-*N*′-methoxy-*N*′-methylamide of alanine (Ala-NOM, Figure 1 **4A**) and its boron isostere (B-Ala-BOM, Figure 1 **4B**) have been adopted as models to study the ϕ and ψ distribution of such peptides. The hypersurfaces of NMA-NOM (Figure 2, **5A**) and BMA-BOM (Figure 2, **5B**), with their associated ground and transition states, and the ground states of Ala-NOM (Figure 1, **4A**) and B-Ala-BOM (Figure 1, **4B**) have been mapped by ab initio Hartree−Fock (HF), density functional, and post-HF methods. Second-order orbital interactions by natural bond orbitals (NBO) method was also carried out to understand the fundamental differences in the structures of the *N*-methoxy peptides and their boron isosteres.

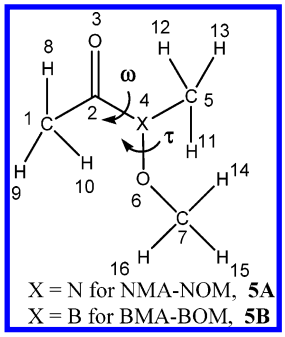

Figure 2. Structures and atomic numbering of NMA-NOM and BMA-BOM.

Computational Details

Ab initio molecular orbital[19] and density functional theory[20] calculations have been carried out using the Gaussian03W[21] (revision C.01) package running on a Pentium III processor with 512 MB RAM. The stability of all wave functions was checked at the HF,[22] Becke's three parameter exchange functional and the gradient corrected functional of Lee, Yang, and Paar (B3LYP)[23−25] and second-order Møller−Plesset MP2 (full)[26,27] level of theory using the 6-31+G* basis set.

The atom labels for NMA-NOM (Figure 2, **5A**) and BMA-BOM (Figure 2, **5B**) are listed in Figure 2, and the two torsion angles, ω and τ, are defined as shown in Figure 1. In NMA-NOM, the methoxy moiety can adopt two conformations around the N−O bond. In the first, the two lone pairs of electrons of O are both *syn-clinal* and in the second, both *anti-clinal* with respect to the lone pair of electrons on N. This has been observed from a conformational search of methoxyamine by ab initio calculations. These initial two conformations around the N−O bond in NMA-NOM were chosen, and for each such arrangement of τ, a scan in increments of 30° of the ω torsion angle was carried out at the HF/6-31+G* level of theory. Conformations with an ω value of 30° and 210° were found to be the lowest in energy. Now, for each conformation with ω value of 30° and 210°, respectively, a τ scan in increments of 30° was run at the HF/6-31+G* level of theory. The minima and saddle points for rotations about the ω and τ torsions were thus identified. All these conformations were further optimized at the B3LYP and MP2 levels of theory with the same basis set, and the conformations were confirmed by frequency calculations, which returned one imaginary frequency for each transition state and all positive frequencies for each ground state. The

Table 1. Energies (au) and Relative Energies (kcal/mol) of Various Minima and Transition States on PES of NMA-NOM (**5A**)[d]

				HF/6-31+G*		B3LYP/6-31+G*		MP2/aug-cc-pVDZ//MP2/6-31+G*			
		NIMAG	PG	au[a]	rel[b]	au[a]	rel[b]	au	rel[b]	ω[c]	τ[c]
minima	GM	0	C_1	−360.692065	0.0	−362.8731751	0.0	−362.0266299	0.0	202	121
	LM	0	C_1	−360.686262	3.6	−362.8679049	3.3	−362.0222521	2.7	34	92
ω rotation transition state (TS)	ωTS1	1	C_1	−360.670192	13.7	−362.8497351	14.7	−362.0053375	13.4	124/−124	127/−127
	ωTS2	1	C_1	−360.662019	18.8	−362.8434716	18.6	−361.9990177	17.3	117/−117	−74/74
	ωTS3	1	C_1	−360.669763	14.0	−362.8499436	14.6	−362.0062633	12.8	41/−41	−104/104
	ωTS4	1	C_1	−360.649892	26.5	−362.8330564	25.2	−361.9889636	23.6	49/−49	88/−88
τ rotation TS	τTS1	1	C_1	−360.674862	10.8	−362.8597467	8.4	−362.010931	9.9	−165	−151
	τTS2	1	C_1	−360.661238	19.3	−362.8492256	15.0	−362.0017625	15.6	179	21
	τTS3	1	C_1	−360.663241	18.1	−362.8492949	15.0	−362.0028588	14.9	32	−148
	τTS4	1	C_1	−360.669256	14.3	−362.8552055	11.3	−362.0073941	12.1	19	6

[a] Zero-point vibrational energy corrected values. [b] Relative energy in kcal/mol. [c] Torsion angle in degrees. [d] NIMAG = number of imaginary frequency, PG = point group, GM = global minimum, LM = local minimum.

MP2/aug-cc-pVDZ calculations were carried out on all minima and transition states optimized at the MP2/6-31+G* level of theory.

A similar strategy was adopted for probing the conformational space of BMA-BOM. The methoxyborane moiety has a planar conformation, and the resulting τ angles in BMA-BOM are either 0° or 180°. The two BMA-BOM conformations with τ values of 0° and 180° were each examined by an ω scan in increments of 30° at the HF/6-31+G* level of theory. With a τ value of 0°, structures with ω of 60°/−60° were found to be the minima, while with a τ value of 180°, the structure with ω of 180° was found to be the minimum. The two conformations with ω values of 60° and 180° were then evaluated by a τ scan in increments of 30° at the HF/6-31+G* level of theory. The minima and saddle points for rotations around the ω and τ angles were thus located. All these structures were further optimized at the B3LYP and MP2 levels of theory using the 6-31+G* basis set and the minima and saddle points confirmed by frequency calculations. The MP2/aug-cc-pVDZ calculations were carried out on all minima and transition states optimized at the MP2/6-31+G* level of theory.

The NBO[28−30] analysis was carried out on the minimum energy structures of NMA-NOM (Figure 2, **5A**) and BMA-BOM (Figure 2, **5B**), optimized at the MP2(full)/6-31+G* level, to quantitatively estimate the second-order interactions as $E_{ij} = -2F_{ij} / \Delta E_{ij}$, where E_{ij} is the energy of the second-order interaction; $\Delta E_{ij} = E_i - E_j$ is the energy difference between the interacting molecular orbitals i and j; and F_{ij} is the Fock matrix element for the interaction between orbitals i and j. The "atomic partial charges" of the global minimum of NMA-NOM (**5A**) and BMA-BOM (**5B**), optimized at the MP2(full)/6-31+G* level, were calculated using natural population analysis (NPA) as implemented in NBO and additionally by the 'ESP fit' method formulated by Merz, Singh, and Kollman.[31]

For Ala-NOM (Figure 1, **4A**), the minima in the ϕ and ψ space was searched starting with two different conformations for ω and τ as identified (Table 1) previously for NMA-NOM (**5A**). This corresponds to structures with $\omega = 202°$; $\tau = 120°$ and $\omega = 34°$; $\tau = 92°$. For each (ω, τ) pair, 144 conformations were generated with 30° increments of the ϕ, ψ dihedrals. Each conformation was geometry optimized first at the HF/3-21G level of theory with "constraints" on the initial ϕ, ψ angles. A Ramachandran map of the 144 conformations was constructed, and conformations within 5.0 kcal/mol of the global minimum were identified. These low-energy conformations were further optimized without constraints at the B3LYP/6-31+G* level of theory. A similar study was carried out for B-Ala-BOM (**4B**) with the starting (ω, τ) pairs of (67°, 0°) and (165°, 181°).

Results and Discussion

All wave functions for molecules **4A**, **4B**, **5A**, and **5B** (Figures 1 and 2) were found to be stable under the perturbations considered at the HF, B3LYP, and MP2 levels of theory.

Minima and Saddle Points of NMA-NOM (5A). For NMA-NOM (**5A**) besides the global minimum (GM), there is also a local minimum (LM) at 2.7 kcal/mol of the GM. For each structure, several transition states (TS) for rotation about the ω angle exists. The geometries of these TS depend on the state of the pyramidal amide nitrogen, i.e. the lone pair of electrons on nitrogen may either be directed downward which is labeled as 'pyramidal up', or the lone pair of electrons on nitrogen may be positioned upward which is labeled as 'pyramidal down'. This is further complicated by the orientation of the two lone pairs of electrons on the methoxy oxygen relative to the lone pair on the amide nitrogen. In all, four transition states can be identified for 'ω rotation' taking into consideration all positions of the lone pair of electrons on the amide nitrogen and methoxy oxygen atoms.

Further, proceeding from the GM and LM structures four TS corresponding to rotation about the τ angle have been identified. The transition states τTS1 and τTS2 are the rotation barriers for the τ angle in the GM, while the transition states τTS3 and τTS4 are for the LM. In summation, a total of eight TS have been identified on the potential energy surface of NMA-NOM (**5A**). The energies of the minima and TS at the HF, B3LYP, and MP2 levels of theory are listed in Table 1. The geometries of the minima and TS have been pictorially depicted in Figure 4, and the geometrical data (bond lengths, bond angles, and torsion angles) are given in Table 3.

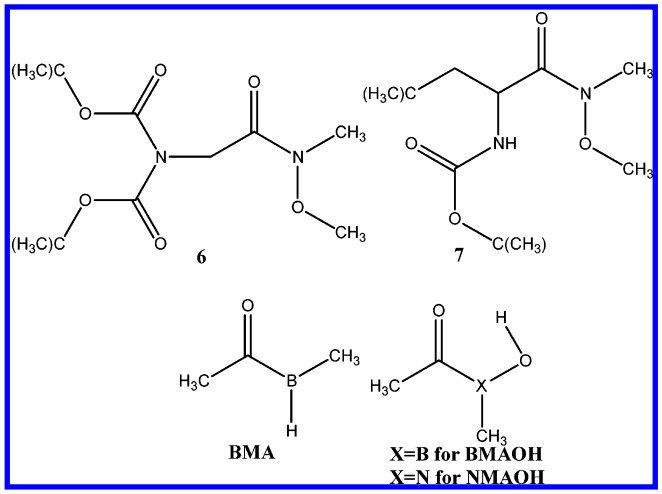

Figure 3. Structures of BMA, BMAOH, NMAOH, and *N*-methoxy peptides (**6** and **7**).

All structures exhibit C_1 symmetry. There is a small increase of about 0.06−0.07 Å in the C(O)−N bond length in the transition states for rotation about the ω angle compared to the two ground states (GM and LM). Kosturkiewicz et al.[32] have reported the X-ray crystal structure of *N*,*N*-di-*tert*-butyloxycarbonyl-glycin-*N*′-methoxy-*N*′-methylamide (Figure 3, **6**), and Kolter et al.[33] have reported the X-ray crystal structure of 2(*S*)-*N*-*tert*-butoxycarbonylamino-*N*-methoxy-*N*-methylbutanamide (Figure 3, **7**). In both these structures the NMA-NOM segment has close resemblance to the GM of NMA-NOM. The geometric parameters of these two structures have been compared in Table 4 with the calculated parameters for NMA-NOM (**5A**). Thus, the bond lengths and bond angles of NMA-NOM at the MP2-(full)/6-31+G* level of theory are close to those in the crystal structures mentioned above around the *N*-methoxy amide region. The ω angle is found to be 202° and 34° in the global and local minimum structures of NMA-NOM (**5A**), while this torsion in *N*,*N*-dimethylacetamide[34] (a model for *N*-methyl peptides), *N*-methylacetamide[35] (a model for natural peptides), and in natural peptides and proteins is found to be ca. 180° and ca. 0° for the corresponding global and local energy minimum structures, respectively. The nitrogen in NMA-NOM is pyramidal, while that in natural peptide is planar. The deviation of amide bond from planarity in NMA-NOM is a consequence of the electronegativity of the hydroxy group attached to nitrogen in addition to the steric effect of the methoxy group. The deviation in the ω angle in NMA-NOM (**5A**), from that found in natural peptides, subsequently affects the ϕ, ψ distributions in *N*-methoxy peptides. The transition states for ω rotation in NMA-NOM (**5A**) has a structural pattern in the amide bond (pyramidal nitrogen with the lone pair of electrons either *syn-* or *anti*-periplanar to the carbonyl group) similar to that seen in the transition states for ω rotation of *N*-methylacetamide.[36]

Minima and Saddle Points of BMA-BOM (5B). The potential energy surface of BMA-BOM (**5B**) is characterized by two minima—the global minimum (GM) and a local minimum (LM); three transition states for rotation about the ω angle ωTS1 to ωTS3; and one transition state for rotation about the τ angle (τTS). Boron adopts a planar structure unlike pyramidal for N in NMA-NOM (**5A**). The conformations of the ground and TS of BMA-BOM are shown in Figure 5, and the absolute and relative energies at the HF, B3LYP, and MP2(full) levels of theory with the 6-31+G* basis set are given in Table 2. The GM, LM, and the structure corresponding to the transition state for τ rotation (τTS) exhibit a C_1 symmetry, while all the three transition states for ω rotation (ωTS1 to ωTS3) exhibit a C_s symmetry. In the ground-state structures, the ω and τ values in the GM are 165° and 181°, while in the LM they are 67° and 0°, respectively. In comparison, the ω and τ values in the GM of NMA-NOM (**5A**) are 202° and 121° and in the LM they are 34° and 92°, respectively. The minima of NMA-NOM and BMA-BOM exhibit significant conformational differences. In the transition state for ω rotation (ωTS1) the ω and τ angles have values of 0° and 180°; in ωTS2 they are 0° and 0°, while in ωTS3 they are 180° and 0°, respectively. In the case of the transition state corresponding to rotation

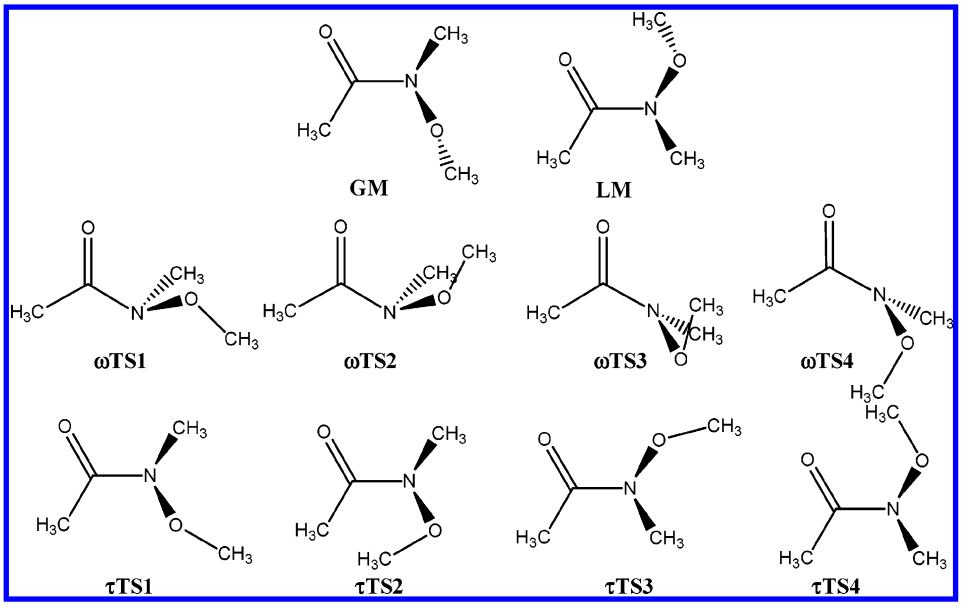

Figure 4. Ground and transition states of NMA-NOM (**5A**).

Table 2. Energies (au) and Relative Energies (kcal/mol) of Various Minima and Transition States on PES of BMA-BOM (**5B**)[d]

				HF/6-31+G*		B3LYP/6-31+G*		MP2/aug-cc-pVDZ//MP2/6-31+G*			
		NIMAG	PG	au[a]	rel[b]	au[a]	rel[b]	au	rel[b]	ω[c]	τ[c]
minima	GM	0	C_1	−331.036343	0.0	−333.0720115	0.0	−332.2595155	0.0	165	181
	LM	0	C_1	−331.0346427	1.1	−333.0709604	0.7	−332.2583229	0.7	67	0
ω rotation TS	ωTS1	1	C_s	−331.029499	4.3	−333.0660019	3.8	−332.2536856	3.7	0	180
	ωTS2	1	C_s	−331.0321876	2.6	−333.0686721	2.1	−332.256573	1.8	0	0
	ωTS3	1	C_s	−331.0269482	5.9	−333.0637057	5.2	−332.251972	4.7	180	0
τ rotation TS	τTS	1	C_1	−331.0202402	10.1	−333.0542493	11.1	−332.237326	13.9	−98/98	85/−85

[a] Zero-point vibrational energy corrected values. [b] Relative energy in kcal/mol. [c] Torsion angle in degrees. [d] NIMAG = number of imaginary frequency, PG = point group, GM = global minimum, LM = local minimum.

Table 3. Bond Length (Å) and Bond Angles (deg) of NMA-NOM (**5A**) Optimized at the MP2(full)/6-31+G* Level

parameter	GM	LM	ωTS1	ωTS2	ωTS3	ωTS4	τTS1	τTS2	τTS3	τTS4
CC (1,2)	1.506	1.513	1.498	1.497	1.506	1.514	1.505	1.512	1.517	1.519
CO (2,3)	1.233	1.230	1.218	1.223	1.220	1.219	1.238	1.240	1.230	1.238
CN (2,4)	1.393	1.394	1.473	1.461	1.464	1.461	1.380	1.389	1.390	1.369
NC (4,5)	1.457	1.457	1.467	1.461	1.460	1.453	1.452	1.457	1.456	1.452
NO (4,6)	1.421	1.416	1.459	1.445	1.464	1.448	1.443	1.446	1.438	1.429
OC (6,7)	1.434	1.435	1.430	1.443	1.435	1.437	1.427	1.425	1.425	1.442
CCO (1,2,3)	123.5	122.7	125.3	124.7	123.5	121.2	123.3	119.7	122.1	121.0
CCN (1,2,4)	116.3	115.3	112.4	112.3	118.2	120.7	116.3	121.3	115.0	114.5
CNC (2,4,5)	118.6	122.4	109.6	112.0	114.4	116.3	119.6	117.1	121.4	125.1
CNO (2,4,6)	113.2	113.2	103.6	108.0	101.1	106.8	112.0	126.2	109.6	124.7
CNO (5,4,6)	111.1	108.3	105.7	112.5	105.4	113.5	120.1	104.2	118.2	105.0
NOC (4,6,7)	108.7	109.1	107.2	117.5	107.4	116.7	114.7	119.0	115.6	119.0
CCNC (ω) (1,2,4,5)	202.5	33.6	124.1	116.7	41.0	48.4	195.0	179.4	31.7	18.6
CCNO (1,2,4,6)	335.3	166.0	236.5	241.0	288.3	280.7	343.5	315.1	175.3	169.0
CNOC (τ) (2,4,6,7)	121.1	92.2	127.0	285.8	255.7	88.3	209.3	20.9	212.0	6.4
OCNC (3,2,4,5)	25.2	209.3	304.0	296.0	218.8	227.0	18.4	8.9	207.7	294.8

Table 4. Geometric Parameters of GM of NMA-NOM at the MP2(full)/6-31+G* Level of Theory and X-ray Crystal Structures of *N,N*-Di-*tert*-butyloxycarbonyl-glycin-*N*′-methoxy-*N*′-methylamide and 2(*S*)-*N*-*tert*-Butoxycarbonylamino-*N*-methoxy-*N*-methylbutanamide

parameter	GM	*N,N*-di-*tert*-butyl-oxycarbonyl-glycin-*N*′-methoxy-*N*′-methylamide (**6**)	2(*S*)-*N*-*tert*-butoxy-carbonylamino-*N*-methoxy-*N*-methyl-butanamide (**7**)
CC (1,2)	1.506	1.505	1.530
CO (2,3)	1.233	1.212	1.223
CN (2,4)	1.393	1.351	1.357
NC (4,5)	1.457	1.450	1.453
NO (4,6)	1.421	1.390	1.404
OC (6,7)	1.434	1.418	1.453
CCO (1,2,3)	123.5	123.2	123.2
CCN (1,2,4)	116.3	115.3	116.4
CNC (2,4,5)	118.6	124.0	123.5
CNO (2,4,6)	113.2	115.7	117.8
CNO (5,4,6)	111.1	115.4	114.3
NOC (4,6,7)	108.7	110.7	109.7
CCNC (ω) (1,2,4,5)	202.5	191.6	200.61
CCNO (1,2,4,6)	335.3	344.7	354.3
CNOC (τ) (2,4,6,7)	121.1	114.1	109.7
OCNC (3,2,4,5)	25.2	12.1	17.6

of the τ angle (τTS), the values of both the torsion angles (ω and τ) are ∼90°.

The geometric parameters of the minima and all transition states of BMA-BOM (**5B**) at the MP2(full)/6-31+G* level of theory are given in Table 5. The changes in the bond lengths from the ground to the TS are relatively small. Some geometric parameters for alkylboranes, arylboranes, and borane complexes have been reported, but there are no experimental data for acylboranes such as BMA[14] (Figure 3) and BMAOH[15] (Figure 3). We had earlier reported the geometry of BMA (Figure 3) which is the boron isostere of *N*-methylacetamide, at the QCISD/6-31G* level of theory.[14] The B−O bond length in BMAOH (Figure 3) is 1.356 Å in the GM and 1.369 Å in the LM at the MP2(full)/6-31+G*

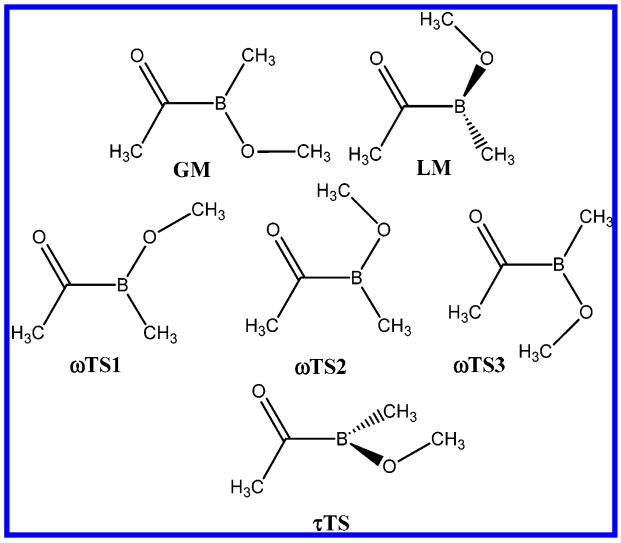

Figure 5. Ground and transition states of BMA-BOM (**5B**).

Table 5. Bond Length (Å) and Bond Angles (deg) of BMA-BOM (**5B**) Optimized at the MP2(full)/6-31+G* Level

parameter	GM	LM	ωTS1	ωTS2	ωTS3	τTS
CC (1,2)	1.509	1.508	1.518	1.511	1.514	1.502
CO (2,3)	1.244	1.245	1.199	1.244	1.244	1.249
CB (2,4)	1.612	1.605	1.639	1.627	1.632	1.592
BC (4,5)	1.568	1.569	1.588	1.573	1.566	1.567
BO (4,6)	1.362	1.358	1.334	1.353	1.361	1.381
OC (6,7)	1.437	1.441	1.405	1.442	1.433	1.429
CCO (1,2,3)	120.7	120.9	119.9	119.7	118.5	121.9
CCB (1,2,4)	120.3	121.8	119.9	119.3	125.9	127.4
CBC (2,4,5)	122.0	120.7	121.0	120.8	117.5	122.5
CBO (2,4,6)	113.4	120.3	114.1	121.8	125.6	115.5
CBO (5,4,6)	124.5	118.9	124.9	117.3	116.9	121.8
BOC (4,6,7)	121.4	121.9	125.9	126.8	128.2	123.8
CCBC (ω) (1,2,4,5)	165.0	66.7	0.0	0.0	180.0	262.8
CCBO (1,2,4,6)	345.3	244.4	180.0	180.0	0.0	83.7
CBOC (τ) (2,4,6,7)	180.8	0.6	180.0	0.0	0.0	84.7
OCBC (3,2,4,5)	344.3	249.8	180.0	180.0	0.0	85.6

level of theory.[15] The B−O bond length in BMA-BOM (**5B**) is found to be 1.362 Å in the GM and 1.358 Å in the LM structures (Table 5) at the MP2(full)/6-31+G* level of theory. The B−O bond length, reported in the literature for a range of organic and inorganic boron containing molecules, varies from 1.34 to 1.42 Å (average 1.38 Å) for boron with trigonal planar geometry and 1.39 to 1.52 Å (average 1.48 Å) for boron with tetrahedral geometry.[37,38] The B−O bond length for BMA-BOM calculated in this study is in the range of the experimental values. The NBO calculations on the minimum energy structure of BMA-BOM at the MP2(full)/6-31+G* level of theory reveals a double bond character for the B−O bond, and the second B−O bond has an occupancy of 1.99 (∼2.0) electrons with contribution from one of the lone pairs of electrons of oxygen. In alkylboranes, the B−C (aliphatic carbon) bond length is about 1.590 Å as in for e.g. dimethylborane,[39] 1.596 Å in dimesitylborane,[40] 1.570 Å in ditripylborane,[41] 1.571 Å in BMA,[14] and 1.564 Å in BMAOH.[15] The B4−C5 bond length in BMA-BOM is 1.57 Å, which comes near to the experimental value for the aliphatic carbon−boron bond.

Rotation Barrier in NMA-NOM (5A) and BMA-BOM (5B). The barrier to rotation about the ω angle in the natural peptide ranges from 16.0 to 25.0 kcal/mol,[36] while that for the boron isostere is only about 5.0 kcal/mol.[14] The boron analogues are thus relatively more flexible than the natural peptides. In case of the *N*-methoxy peptides and the corresponding boron isosteres, there are two rotation barriers governed by the ω and τ angles. In the example of NMA-NOM (**5A**), the ω rotation barrier is relatively higher (12.8−23.6 kcal/mol) than the τ rotation barrier (9.9−15.6 kcal/mol). In BMA-BOM (**5B**), the τ rotation barrier is comparatively higher (13.9 kcal/mol) than its ω rotation barrier (1.8−4.7 kcal/mol). The relative higher τ rotation barrier in boron peptides is a consequence of the B−O double bond character as revealed by NBO calculations. The heights of the rotation barriers seen for the methoxy peptides (NMA-NOM and BMA-BOM) is similar to that for the hydroxyl peptides (NMAOH and BMAOH, Figure 3) reported earlier.[15]

The rotation barrier in amide systems (like peptides, urea, guanidine, etc.) has been attributed to delocalization of the lone pair of electrons on nitrogen onto the C−N bond as explained by the classical resonance model.[42] This explanation imparts a partial double bond character to the C−N bond. But recent experimental and theoretical studies[43−47] reveal that the electron delocalization in the amide system has been attributed to second-order orbital interactions namely, $n_O \rightarrow \sigma^*_{C-N}$ (delocalization from lone pairs on carbonyl oxygen into the sigma antibonding orbital of the C−N bond i.e. negative hyperconjugation) and $n_N \rightarrow \pi^*_{C-O}$ (delocalization from the lone pair on amide nitrogen to the pi antibonding orbital of the carbonyl group). The energy $E^{(2)}$ associated with negative hyperconjugation i.e. $n_O \rightarrow \sigma^*_{C-N}$ is 34.8 kcal/mol (occupancy of n_O is 1.906 and σ^*_{C-N} is 0.070) and that with $n_N \rightarrow \pi^*_{C-O}$ is 58.0 kcal/mol (occupancy of n_N is 1.827 and π^*_{C-O} is 0.170) for the global minimum of NMA-NOM at the MP2(full)/6-31+G* level. In case of BMA-BOM, the energy associated with negative hyperconjugation i.e. $n_O \rightarrow \sigma^*_{C-B}$ is only 13.4 kcal/mol (occupancy of n_O is 1.941 and σ^*_{C-B} is 0.036), indicating that the C−B bond delocalization is insignificant, as a result of which, the rotation barrier in boron peptide is very small. Thus, in BMA-BOM, the C−B bond has an essentially single bond character, while the C−N bond in NMA-NOM has a larger double bond character. The boron analogues are thus far more flexible than the *N*-methoxy peptides. The second-order orbital interactions closely parallel that for the corresponding *N*-hydroxy peptides reported earlier.[15] The energy associated with negative hyperconjugation i.e. $n_O \rightarrow \sigma^*_{C-N}$ is 32.8 kcal/mol and that with $n_N \rightarrow \pi^*_{C-O}$ is 98.5 kcal/mol for the global energy minimum structure of *N*-methylacetamide.[13] Thus, the $n_N \rightarrow \pi^*_{C-O}$ electron delocalization is reduced significantly when N−H bond in natural peptide (*N*-methylacetamide) is replaced by N−OCH_3 (NMA-NOM, **5A**). This is probably due to the fact that the electronegative oxygen withdraws electrons from the nitrogen atom.

Partial Atomic Charges of NMA-NOM (5A) and BMA-BOM (5B). The "natural charges" derived from NPA for the global minimum energy structure of NMA-NOM (**5A**)

Table 6. Partial Atomic Charges of NMA-NOM (**5A**) and BMA-BOM (**5B**) Calculated Using NPA and the 'ESP Fit' as per Merz−Singh−Kollman Scheme at the MP2(full)/6-31+G* Level

		natural charges		ESP fitted charges	
atom	atom no.	NMA-NOM (**5A**)	BMA-BOM (**5B**)	NMA-NOM (**5A**)	BMA-BOM (**5B**)
C	1	−0.73111	−0.73103	−0.605573	−0.293486
C	2	0.83787	0.33658	0.904859	0.394028
O	3	−0.71280	−0.63221	−0.650117	−0.553132
X	4	−0.29335	1.08601	−0.260075	0.711483
C	5	−0.41351	−1.07467	−0.318880	−0.587438
O	6	−0.49098	−0.83597	−0.244952	−0.519024
C	7	−0.23095	−0.23724	−0.119883	0.032558
H	8	0.25241	0.24135	0.153101	0.113004
H	9	0.24073	0.23748	0.180700	0.067244
H	10	0.25758	0.24544	0.180506	0.069023
H	11	0.21366	0.24032	0.149242	0.126094
H	12	0.21753	0.24612	0.155416	0.127817
H	13	0.25216	0.27020	0.159344	0.114528
H	14	0.19358	0.19508	0.075715	0.050418
H	15	0.19566	0.19846	0.117315	0.064449
H	16	0.21151	0.21406	0.123283	0.082434

and BMA-BOM (**5B**) are given in Table 6. Replacement of nitrogen by boron decreases the positive charge on the carbonyl carbon and increases the negative charge on the C5 methyl carbon. In BMA-BOM (**5B**), the boron atom has a much greater positive charge than the carbonyl carbon (1.086 vs 0.336). The site for nucleophilic attack in case of NMA-NOM (**5A**) is normally the carbonyl carbon. In BMA-BOM (**5B**), a nucleophile will preferentially attack boron rather than the carbonyl group. This preference for boron as the site for nucleophilic attack is also evident in the 'ESP fitted charges', even though the partial charges differences are of a smaller magnitude. This was the basis of our hypothesis, used to design boron peptides[13,15] as k_{cat} inhibitors of the enzyme serine protease. The hydroxyl group of serine in the active site is the nucleophile which attacks the carbonyl carbon of the amide of the substrate peptide, leading to a final hydrolysis of the substrate. With the boron peptide in the active site, the hydroxyl group of serine would preferentially attack boron instead of the carbonyl carbon and form a tetrahedral covalent complex leading to irreversible inhibition of the enzyme, thus acting as plausible inhibitor of serine protease enzyme. The inhibitors of serine proteases have great potential in therapeutics.[48−54] When the electrophilicity of the carbonyl carbon in NMA-NOM vs that in *N*-methylacetamide is compared,[13] the differences are insignificant based on the NPA charges on carbonyl carbon (0.837 vs 0.862). However, in case of the boron analogues, the electrophilic character of the boron atom is 1.5-fold higher in BMA-BOM than BMA (Figure 3) (the NPA charges of 1.086 vs 0.669) accentuating the attack of the nucleophile.

PES of Ala-NOM (4A). The preferred values of the ω and τ angles found in NMA-NOM (**5A**) were introduced into Ala-NOM (**4A**) and the (ϕ, ψ) space of Ala-NOM scrutinized (Table 7). With an *omega* value of 30° and a *tau* value of 90°, the global minimum corresponds to a structure with $\phi = 55°$ and $\psi = 35°$ (Figure 6a). These are close to the values for a left-handed alpha helix ($\phi = 57°$, $\psi = 47°$). The local minimum energy structure has $\phi = -150°$ and $\psi = 30°$ (Figure 6b). These two structures fall in the "allowed regions" of the Ramachandran map. All minimum energy structures are distinguished by the presence of an intramolecular hydrogen bond (Figure 6a,b). The GM structure is characterized by a hydrogen bond between the methoxy O (as acceptor) and the amide NH (as donor), forming a six-membered ring, while the LM structure has a H-bond between the *N*-methoxy N (as acceptor) and the amide NH (as donor), forming a five-membered ring. With an ω angle of 200° and a τ angle of 120°, there is only one favored structure for Ala-NOM (**4A**) with $\phi = -90°$ and $\psi = 80°$. These values are close to that for a residue at the $i+1$ position in a type V β−turn ($\phi = -80°$, $\psi = 80°$). This structure is characterized by only one intramolecular hydrogen bond (Figure 6c) between the carbonyl O (as acceptor), near the methoxy group, and the amide NH (as donor) outlining a seven-membered ring. Thus, all the preferred conformations of Ala-NOM are characterized by the presence of one intramolecular hydrogen bond and are conformationally rigid.

PES of B-Ala-BOM (4B). In a similar manner, the ϕ, ψ preferences of B-Ala-BOM (**4B**) were investigated, and the results are shown in Table 7. With an *omega* value of 165° and a *tau* value of 180°, one conformation is observed within 5.0 kcal/mol of the global minimum energy conformer. The global minimum corresponds to a structure with $\phi = 90°$ and $\psi = -60°$ (Figure 7a), while the local minimum relates to a structure with $\phi = -100°$ and $\psi = 70°$ (Figure 7b). The global minimum shows a strong preference for a positive ϕ value. The GM corresponds to the mirror image of a 2.27 ribbon ($\phi = 78°$, $\psi = -59°$), while the LM corresponds to a 2.27 ribbon ($\phi = -78°$, $\psi = 59°$) structure. The two structures exhibit an intramolecular hydrogen bond (Figure 7a,b) between the carbonyl O (as acceptor) next to the B-methoxy group and the amide NH (as donor), forming a seven-membered ring. With an ω angle of 60° and a τ value of 10°, the global minimum corresponds to a structure with $\phi = -40°$ and $\psi = 120°$ (Figure 7c). These are close to the values adopted by an $i+1$ residue in a type Va β-turn ($\phi = -60°$, $\psi = 120°$ with 'cis' *omega*). The local minimum corresponds to a structure with $\phi = 85°$ and $\psi = 180°$ (Figure 7d). These are near to the values of a poly-L-Pro II helix ($\phi = 79°$, $\psi = 210°$). The next local minimum energy structure has $\phi = 90°$ and $\psi = 100°$ (Figure 7e). The structure is again characterized by a positive ϕ value which is 'disallowed' for natural peptides.

Overview of Boron Peptides. In an earlier paper,[13,14] we had studied the geometries and transition states of boron analogues of the natural peptides. The natural peptides have ω values either 180° or 0°, while the ϕ, ψ torsion angles fall in the 'allowed' regions of the Ramachandran map. The boron analogue (BMA, Figure 3) exhibits an unusual ω value of 90°, and the corresponding Ala-dipeptide exhibits a unique preference for positive ϕ values in the 'disallowed' region of the Ramachandran map but with no regular secondary structure motif. In a subsequent paper,[15] we had investigated the conformational space of the B−OH analogue (BMAOH,

Table 7. Conformations and Energies of Ala-NOM (**4A**) and B-Ala-BOM (**4B**)

	ω	τ	ϕ	ψ	rel *E* (kcal/mol)	structural feature (ideal values of the torsion angles)
Ala-NOM	30°	90°	55°	35°	0.0	left-handed α-helix (57°, 47°)
			−150°	30°	0.3	random
	200°	120°	−90°	80°	0.0	type V β-turn *i*+*1* residue (−80°, 80°)
B-Ala-BOM	165°	180°	90°	−60°	0.0	positive ϕ, mirror image of 2.27 ribbon (78°, −59°)
			−100°	70°	0.3	2.27 ribbon (−78°, 59°)
	60°	10°	−40°	120°	0.0	type Va β-turn *i*+1 residue (−60°, 120°, *cis omega*)
			85°	180°	1.4	positive ϕ, mirror image of Poly-L-Pro II helix (79°, 210°)
			90°	100°	2.2	positive ϕ, folded

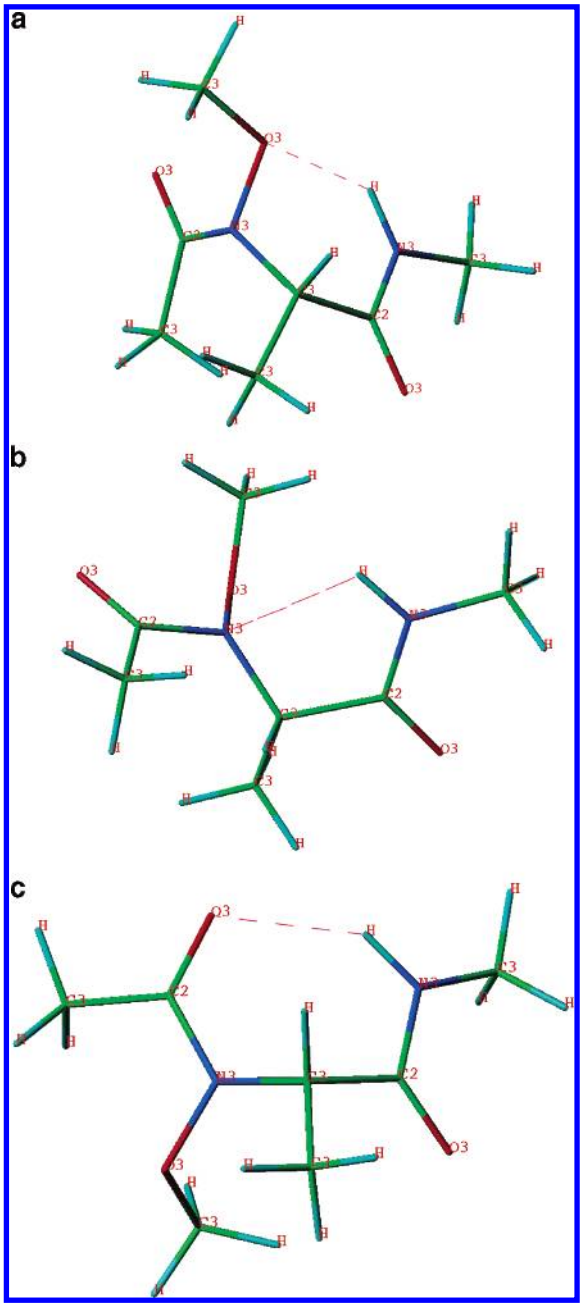

Figure 6. Preferred conformations of Ala-NOM (**4A**): (a) $\omega = 30°$, $\tau = 90°$, $\phi = 55°$, $\psi = 35°$, (b) $\omega = 30°$, $\tau = 90°$, $\phi = -150°$, $\psi = 30°$, and (c) $\omega = 200°$, $\tau = 120°$, $\phi = -90°$, $\psi = 80°$.

Figure 3) and its corresponding peptide with the N−OH moiety. The replacement of the N−H bond (*N*-methylacetamide) by N−OH (NMAOH, Figure 3) shifts the preference for the ω torsion from 180° to 32° due to a strong tendency to form a hydrogen bond within the amide segment. The local energy minimum structure has an ω value of 202°. Similarly modifying the boron analogue by replacement of B−H (BMA, Figure 3) with B−OH (BMAOH, Figure 3) leads to a change in the ω torsion from 90° to 0° and again this is driven by the predisposition to form an intramolecular hydrogen bond. The local energy minimum structure of BMAOH has an ω value of 153°. The intramolecular hydrogen bond imparts conformational rigidity to these peptides. The Ala-dipeptide derived from NMAOH assumes either a type-I beta-turn or a left-handed alpha-helix. The Ala-dipeptide derived from BMAOH shows a leaning toward positive ϕ, and extended ψ values, with no regular secondary structure motifs. In the present class of molecules where the N−H bond is replaced by N−OCH_3 (NMA-NOM, **5A**) and the B−H bond is replaced by B−OCH_3 (BMA-BOM, **5B**), the conformational space of the corresponding peptides is different from the previously reported natural peptides and their hydroxy derivatives. In NMA-NOM (**5A**) the ω values are 202° and 32° in the GM and LM structures, which are near to the structures for the natural peptides. A similar shift in the torsion is also seen in BMA-BOM with a value of 165° for the ω angle. The dipeptides bearing the N−OCH_3 and B−OCH_3 (Figure 1, **4A** and **4B**) moieties have in common the type-V β-turn motif beside adopting several of the regular secondary structures. Thus, it has been observed that modifying the B−H bond as B−OH and further as B−OCH_3 is able to induce a change in the peptide backbone from a random coil-like state to a more ordered secondary structure.

Conclusions

The boron isosteres of the amino acids were designed by replacement of the amide nitrogen with boron,[13] with the intention of developing an irreversible inhibitor of the enzyme serine protease. The synthesis of such a molecule is a big challenge. Based on the strong affinity of boron for oxygen, these analogues were modified to B−OH which are easy to synthesize, and this derivative is echoed in the *N*-hydroxy amides which are well-known. However, from a synthetic standpoint, the methoxy analogues (B−OCH_3) are much more accessible. The conformational space of *N*-methoxy peptides and their boron isosteres has been the focus of investigation in this paper. The minimum in the *omega* torsion space of such molecules has been identified using *N*-methoxy-*N*-methylacetamide (NMA-NOM, **5A**) and acetylmethylmethoxyborane (BMA-BOM, **5B**) as model peptides.

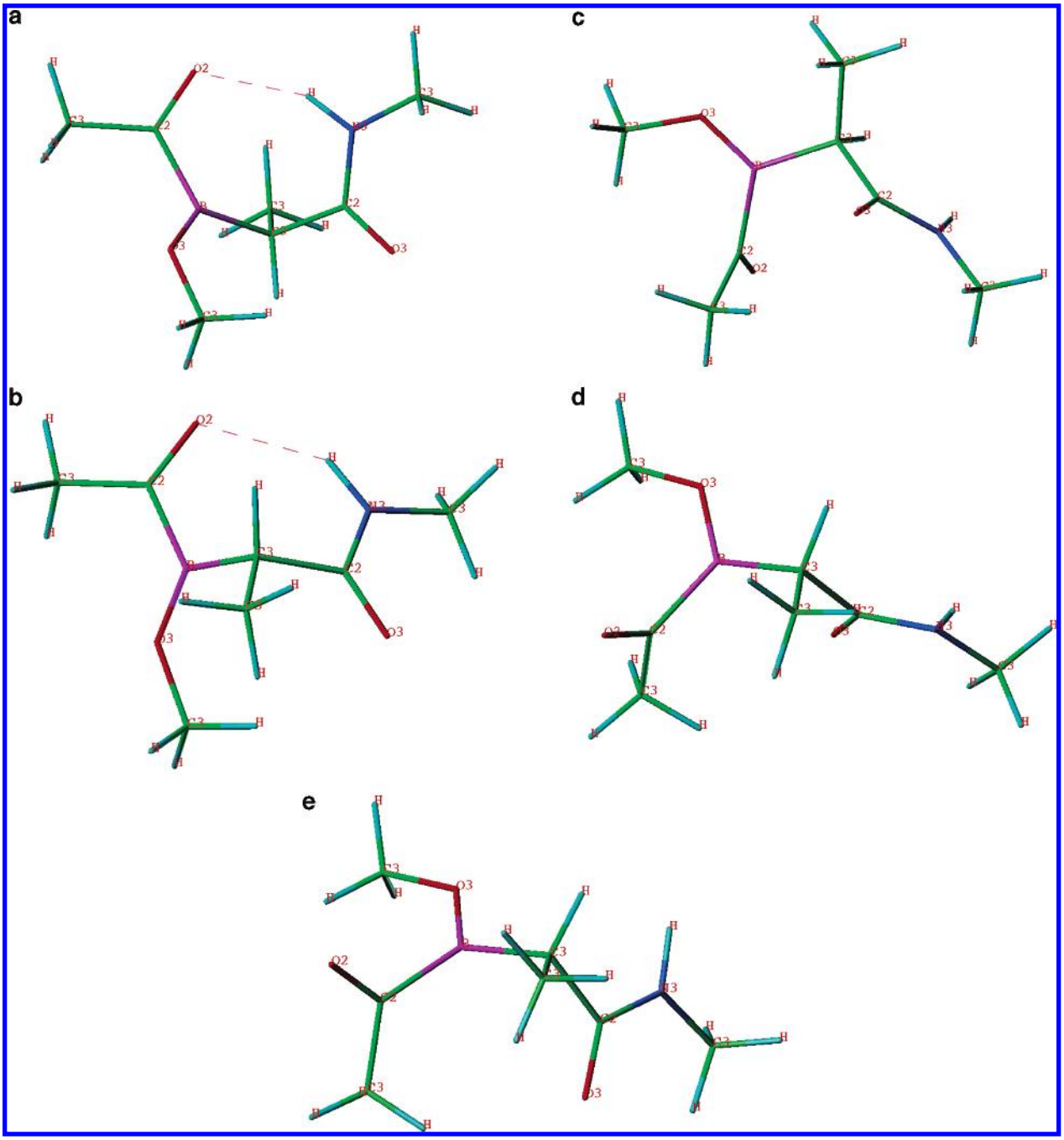

Figure 7. Preferred conformations of B-Ala-BOM (**4B**): (a) $\omega = 165°$, $\tau = 180°$, $\phi = 90°$, $\psi = -60°$, (b) $\omega = 165°$, $\tau = 180°$, $\phi = -100°$, $\psi = 70°$, (c) $\omega = 60°$, $\tau = 10°$, $\phi = -40°$, $\psi = 120°$, (d) $\omega = 60°$, $\tau = 10°$, $\phi = 85°$, $\psi = 180°$, and (e) $\omega = 60°$, $\tau = 10°$, $\phi = 90°$, $\psi = 100°$.

The ground and various transition states for **5A** and **5B** have been calculated at the HF, B3LYP, and MP2(full) levels of theory with the 6-31+G* basis set. The *omega* rotation barrier is seen to be 12.8−23.6 kcal/mol for the *N*-methoxy peptide (NMA-NOM, **5A**) and 1.8−4.7 kcal/mol for its corresponding boron isostere BMA-BOM (**5B**). The difference in the rotation barriers has been attributed to second-order orbital interactions, mainly negative hyperconjugation. The barrier for rotation about the torsion angle τ i.e. rotation about the N−O and B−O bonds is 9.9−15.6 kcal/mol for the *N*-methoxy peptide and 13.9 kcal/mol for the boron isostere. The replacement of nitrogen by boron also significantly changes the charge distribution in these molecules. A relatively greater positive charge on the boron atom over the carbonyl carbon makes boron the preferential site of attack by a nucleophile in boron peptides, which otherwise occurs on the carbonyl carbon in the natural peptides. The minimum energy structures of NMA-NOM and BMA-BOM were then used to study the ϕ and ψ preferences in *N*-acetyl-*N*′-methoxy-*N*′-methylamide of alanine (Ala-NOM) and its boron isostere (B-Ala-BOM). Ala-NOM demonstrates conformations with a type-V β-turn and a left-handed α-helix. B-Ala-BOM, on the other hand, favors conformations with a 2.27 ribbon, the mirror image of 2.27 ribbon, a type-Va β-turn, the mirror image of poly-Pro-II helix, and positive ϕ and extended ψ values. In previous work on natural peptides

and their boron isosteres, we had noticed a much lower barrier to rotation about the ω angle, a unique preference for positive *phi* values in the boron analogues and no regular secondary structure observed. The *N*-methoxy peptides and their boron analogues abound with a variety of secondary structural elements. In conclusion, the replacement of nitrogen by boron in natural and *N*-methoxy peptide causes significant changes in the conformational space and electronic properties, and these features can be profitably exploited to design peptides with specific geometries and chemical attributes.

Acknowledgment. This work is supported by the Department of Science and Technology, New Delhi through their FIST program (SR/FST/LS1-163/2003). A.K.M. thanks both the University Grants Commission, New Delhi and the Council of Scientific and Industrial Research, New Delhi, while S.A.K. thanks the Lady Tata Memorial Trust, Mumbai for financial support.

References

(1) Ramachandran, G. N.; Sasisekharan, V. Conformation of Polypeptides and Proteins. *Adv. Protein Chem.* **1968**, *28*, 283−437.

(2) Hagler, T. A.; Leiserowitz, L.; Tuval, M. Experimental and Theoretical Studies of the Barrier to Rotation about N−Cα and Cα-C′ Bonds (ϕ and ψ) in Amides and Peptides. *J. Am. Chem. Soc.* **1976**, *98*, 4600−4612.

(3) Hruby, V. J. Designing Peptide Receptor Agonists and Antagonists. *Nat. Rev. Drug Discovery* **2002**, *1*, 847−858.

(4) Vogen, S. M.; Paczkowski, N. J.; Kirnarsky, L.; Short, A.; Whitmore, J. B.; Sherman, S. A.; Taylor, S. M.; Sanderson, S. D. Differential Activities of Decapeptide Agonists of Human C5a: The Conformational Effects of Backbone N-Methylation. *Int. Immunopharmacol.* **2001**, *12*, 2151−62.

(5) Ye, Y.; Liu, M.; Kao, J. L.; Marshall, G. R. Peptide-bond Modification for Metal Coordination: Peptides Containing Two Hydroxamate Groups. *Biopolymers* **2003**, *71*, 489−515.

(6) Fischer, P. M. The design, synthesis and application of stereochemical and directional peptide isomers: a critical review. *Curr. Protein Pept. Sci.* **2003**, *4*, 339−356.

(7) Baldauf, C.; Günther, R.; Hofmann, H. J. Conformational Properties of Sulphonamido Peptides. *J. Mol. Struct. (THEOCHEM)* **2004**, *675*, 19−28.

(8) Kettner, C. A.; Shenvi, A. B. Inhibition of Serine Protease Leukocyte Elastase, Pancreatic Elastase, Cathepsin G, and Chymotrypsin by Peptide Boronic Acids. *J. Biol. Chem.* **1984**, *259*, 15106−15114.

(9) Kettner, C. A.; Bone, R.; Agard, D. A.; Bachovchin, W. W. Kinetic Properties of the Binding of α-Lytic Protease to Peptide Boronic Acids. *Biochemistry* **1988**, *27*, 7682−7688.

(10) Spielvogel, B. F.; Wojnowich, L.; Das, M. K.; McPhail, A. T.; Hargrave, K. D. Boron Analogs of Amino Acids. Synthesis and Biological Activity of Boron Analogs of Betaine. *J. Am. Chem. Soc.* **1976**, *98*, 5702−5703.

(11) Spielvogel, B. F.; Das, M. K.; McPhail, A. T.; Onam, K. D.; Hall, I. H. Boron Analogs of the alpha.-Amino Acids. Synthesis, X-Ray Crystal Structure, and Biological Activity of Ammonia-Carboxyborane, the Boron Analog of Glycine. *J. Am. Chem. Soc.* **1980**, *102*, 6343−6344.

(12) Miller, M. C.; Sood, A.; Spielvogel, B. F.; Hall, I. H. Synthesis and Antitumor Activity of Boronated Dipeptides containing Aromatic Amino Acids. *Anticancer Res.* **1997**, *5A*, 3299−3306.

(13) Datar, P. A.; Coutinho, E. C. The ϕ, ψ Space of Boron Isosteres of Amino Acids: An Ab Initio Study. *J. Theor. Comput. Chem.* **2004**, *3*, 189−202.

(14) Malde, A. K.; Khedkar, S. A.; Coutinho, E. C.; Saran A. Geometry, Transition States, and Vibrational Spectra of Boron Isostere of *N*-methylacetamide by Ab Initio Calculations. *Int. J. Quantum Chem.* **2005**, *102*, 734−742.

(15) Malde, A. K., Khedkar S. A.; Coutinho, E. C. The ω, ϕ and ψ Space of N-hydroxy-N-methylacetamide and N-acetyl-N′-hydroxy-N′-methylamide of Alanine and their Boron Isosteres. *J. Chem. Theory Comput.* **2006**, *2*, 312−321.

(16) Tsai, G.; Lane, H. Y.; Yang, P.; Chong, M. Y.; Lange, N. Glycine transporter I inhibitor, N-methylglycine (sarcosine), added to antipsychotics for the treatment of schizophrenia. *Biol. Psychiatry* **2004**, *55*, 452−456.

(17) Pritchard, D. L. Sourcing a chemical succession for cyclosporin from parasites and human pathogens. *Drug Discovery Today* **2005**, *10*, 688−691.

(18) Lee, C. H.; Zimmerman, S. S. Calculations of the phi-psi conformational contour maps for N-acetyl alanine N′-methyl amide and of the characteristic ratios of poly-L-alanine using various molecular mechanics forcefields. *J. Biomol. Struct. Dyn.* **1995**, *13*, 201−218.

(19) Hehre, W. J.; Random, L.; Schleyer, P. V. R.; Pople, J. A. In *Ab Initio Molecular Orbital Theory;* Wiley: New York, 1985.

(20) Parr, R. G.; Yang, W. In *Density Functional Theory of Atoms and Molecules*; O.U.P.: New York, 1989.

(21) Frisch, M. J.; Trucks, G. W.; Schlegel, H. B.; Scuseria, G. E.; Robb, M. A.; Cheeseman, J. R.; Montgomery, J. A., Jr.; Vreven, T.; Kudin, K. N.; Burant, J. C.; Millam, J. M.; Iyengar, S. S.; Tomasi, J.; Barone, V.; Mennucci, B.; Cossi, M.; Scalmani, G.; Rega, N.; Petersson, G. A.; Nakatsuji, H.; Hada, M.; Ehara, M.; Toyota, K.; Fukuda, R.; Hasegawa, J.; Ishida, M.; Nakajima, T.; Honda, Y.; Kitao, O.; Nakai, H.; Klene, M.; Li, X.; Knox, J. E.; Hratchian, H. P.; Cross, J. B.; Adamo, C.; Jaramillo, J.; Gomperts, R.; Stratmann, R. E.; Yazyev, O.; Austin, A. J.; Cammi, R.; Pomelli, C.; Ochterski, J. W.; Ayala, P. Y.; Morokuma, K.; Voth, G. A.; Salvador, P.; Dannenberg, J.; Zakrzewski, V. G.; Dapprich, S.; Daniels, A. D.; Strain, M. C.; Farkas, O.; Malick, D. K.; Rabuck, A. D.; Raghavachari, K.; Foresman, J. B.; Ortiz, J. V.; Cui, Q.; Baboul, A. G.; Clifford, S.; Cioslowski, J.; Stefanov, B. B.; Liu, G.; Liashenko, A.; Piskorz, P.; Komaromi, I.; Martin, R. L.; Fox, D. J.; Keith, T.; Al-Laham, M. A.; Peng, C. Y.; Nanayakkara, A.; Challacombe, M.; Gill, P. M. W.; Johnson, B.; Chen, W.; Wong, M. W.; Gonzalez, C.; Pople, J. A. *Gaussian 03, Revision C.01;* Gaussian, Inc.: Wallingford, CT, 2004.

(22) Roothan, C. C. New Developments in Molecular Orbital Theory. *Rev. Mod. Phys.* **1951**, *23*, 69−89.

(23) Becke, A. D. Density functional thermochemistry. III. The role of exact exchange. *J. Chem. Phys.* **1993**, *98*, 5648−5652.

(24) Lee, C.; Yang, W.; Parr, R. G. Development of the Colle-Salvetti Correlation-Energy Formula into a Functional of the Electron Density. *Phys. Rev.* **1988**, *37B*, 785−789.

(25) Perdew, J. P.; Wang, Y. Accurate and simple analytic representation of the electron-gas correlation energy. *Phys. Rev.* **1992**, *45B*, 13244−13249.

(26) Møller, C.; Plesset, M. S. Note on an Approximation Treatment for Many-Electron Systems. *Phys. Rev.* **1934**, *46*, 618−622.

(27) Martin-Head, G.; Pople, J. A.; Frisch, M. J. MP2 Energy Evaluation by Direct Methods. *Chem. Phys. Lett.* **1988**, *153*, 503−506.

(28) Glendening, E. D.; Reed, A. E.; Carpenter, J. E.; Weinhold, F. *NBO Version 3.1*.

(29) Reed, A. E.; Weinstock, R. B.; Weinhold, F. Natural Population Analysis. *J. Chem. Phys.* **1985**, *83*, 735−746.

(30) Reed, A. E.; Weinhold, F.; Curtiss, L. A. Intermolecular interactions from a natural bond orbital, donor−acceptor viewpoint. *Chem. Rev.* **1988**, *88*, 899−926.

(31) Singh, U. C.; Kollman, P. A. An Approach to Computing Electrostatic Charges for Molecules. *J. Comput. Chem.* **1984**, *5*, 129−145.

(32) Lubkowski, J.; Lankiewicz, L.; Kosturkiewicz, Z. Structure of *N*, N-Di-*tert*-butyloxycarbonyl-glycine *N*′-methoxy-*N*′-methylamide. *Acta Crystallogr.* **1992**, *C48*, 1616−1619.

(33) Sawatzki, P.; Mikeska, T.; Nieger, M.; Hupfer, H.; Kolter, T. 2(*S*)-*N*-*tert*-butoxycarbonylamino-*N*-methoxy-*N*-methylbutanamide. *Acta Crystallogr.* **2002**, *E58*, o1415−o1417.

(34) Suzuki, H.; Ishiguro, S. *N*,*N*-Dimethylacetamide complex of aluminium(III) perchlorate. *Acta Crystallogr.* **2006**, *E62*, m576−m578.

(35) Kang, Y. K. Ab initio MO and density functional studies on *trans* and *cis* conformers of *N*-methylacetamide. *J. Mol. Struct. (THEOCHEM)* **2001**, *546*, 183−193.

(36) Villani, V.; Alagona, G.; Ghio, C. Ab Initio Studies on N-Methylacetamide. *Mol. Eng.* **1999**, *8*, 135−153.

(37) Filatov, S.; Shepelev, Y.; Bubnova, R.; Sennova, N.; Egorysheva, A. V.; Kargin, Y. F. The study of $Bi_3B_5O_{12}$: synthesis, crystal structure and thermal expansion of oxoborate $Bi_3B_5O_{12}$. *J. Solid State Chem.* **2004**, *177*, 515−522.

(38) Shishkov, I. F.; Khristenko, L. V.; Rudakov, F. M.; Vilkov, L. V.; Karlov, S. S.; Zaitseva, G. S.; Samdal, S. The molecular structure of boratrane determined by gas electron diffraction and quantum mechanical calculations. *J. Mol. Struct.* **2002**, *641*, 199−205.

(39) Vijay, A.; Sathyanarayana, D. N. Effects of Basis Set and Electron Correlation on the Structure and Vibrational Spectra of Diborane. *J. Mol. Struct.* **1995**, *351*, 215−229.

(40) Entwistle, C. D.; Marder, T. B.; Smith, P. S.; Howard, A. K.; Fox, M. A.; Mason, S. A. Dimesitylborane monomer-dimer equilibrium in solution, and the solid-state structure of the dimer by single-crystal neutron and X-ray diffraction. *J. Organomet. Chem.* **2003**, *680*, 165−172.

(41) Bartlett, R. A.; Rasikadis, H. V.; Olmstead, M. M.; Power, P. P.; Weese, K. J. Synthesis of the Monomeric $HBtrip_2$ (trip − 2,4,6-iso-$Pr_3C_6H_2$) and the X-ray Crystal Structures of $[HBMes_2]_2$ (Mes = 2,4,6,-$Me_3C_6H_2$) and $HBtrip_2$. *Organometallics* **1990**, *9*, 146−150.

(42) Pauling, L. *In The Nature of Chemical Bond*; Cornell University Press: Ithaca, NY, 1960.

(43) Bharatam, P. V.; Iqbal, P.; Malde, A.; Tiwari, R. Electron Delocalization in Aminoguanidines: A Computational Study. *J. Phys. Chem.* **2004**, *108*, 10509−10517.

(44) Bharatam, P. V.; Moudgil, R.; Kaur, D. Electron Delocalization in Isocyanates, Formamides, and Ureas: Importance of Orbital Interactions. *J. Phys. Chem.* **2003**, *107*, 1627−1634.

(45) Glendening, E. D.; Hrabal, J. A., II. Resonance in Formamide and Its Chalcogen Replacement Analogues: A Natural Population Analysis/Natural Resonance Theory Viewpoint. *J. Am. Chem. Soc.* **1997**, *119*, 12940−12946.

(46) Lauvergnat, D.; Hiberty, P. C. Role of Conjugation in the Stabilities and Rotational Barriers of Formamide and Thioformamide. An ab initio Valence-Bond Study. *J. Am. Chem. Soc.* **1997**, *119*, 9478−9482.

(47) Wiberg, K. B.; Rush, D. J. Solvent Effects on the Thioamide Rotational Barrier: An Experimental and Theoretical Study. *J. Am. Chem. Soc.* **2001**, *123*, 2038−2046.

(48) Hedstrom, L. Serine protease mechanism and specificity. *Chem. Rev.* **2002**, *102*, 4501−4524.

(49) Lebeurrier, N, Vivien, D.; Ali, C. The complexity of tissue-type plasminogen activator: can serine protease inhibitors help in stroke management? *Expert Opin. Ther. Targets* **2004**, *8*, 309−320.

(50) Syrovets, T.; Simmet, T. Novel aspects and new roles for the serine protease plasmin. *Cell Mol. Life Sci.* **2004**, *61*, 873−885.

(51) Simonet, G.; Claeys, I.; Franssens, V, De Loof, A.; Broeck, J. V. Genomics, evolution and biological functions of the pacifastin peptide family: a conserved serine protease inhibitor family in arthropods. *Peptides* **2003**, *24*, 1633−1644.

(52) Roesenblum, J. S.; Kozarich, J. W. Prolyl peptidases: a serine protease subfamily with high potential for drug discovery. *Curr. Opin. Chem. Biol.* **2003**, *7*, 496−504.

(53) Waxler, B.; Rabito, S. F. Aprotinin: a serine protease inhibitor with therapeutic actions: its interaction with ACE inhibitors. *Curr. Pharm. Des.* **2003**, *9*, 777−787.

(54) Narjes, F.; Koch, U.; Steinkuhler, C. Recent developments in the discovery of hepatitis C virus serine protease inhibitors—towards a new class of antiviral agents? *Expert Opin. Invest. Drugs* **2003**, *12*, 153−163.

CT600192G